A Mathematical Model of a Thermally Activated Roof (TAR) Cooling System Using a Simplified RC-Thermal Model with Time Dependent Supply Water Temperature.

Dr. Khalid Ahmed Joudi
Professor
College of Engineering-University of Baghdad, Baghdad
email: khalid47joudi@yahoo.com

Kamal Mohammed Ali
PhD student
College of Engineering-University of Baghdad, Baghdad
email: al_ssafar2005@yahoo.com

ABSTRACT

This paper presents a computer simulation model of a thermally activated roof (TAR) to cool a room using cool water from a wet cooling tower. Modeling was achieved using a simplified 1-D resistance-capacitance thermal network (RC model) for an infinite slab. Heat transfer from the cooling pipe network was treated as 2-D heat flow. Only a limited number of nodes were required to obtain reliable results. The use of 6^{th} order RC-thermal model produced a set of ordinary differential equations that were solved using MATLAB - R2012a. The computer program was written to cover all possible initial conditions, material properties, TAR system geometry and hourly solar radiation. The cool water supply was considered time dependent with the variation of the ambient wet bulb temperature. Results from RC-thermal modeling were compared with experimental measurements for a second story room measuring 5.5 m x 4 m x 3 m at Amarah city/ Iraq (31.865 ˚N, 47.128 ˚E) for 21 July, 2013. The roof was constructed of 200 mm concrete slab, 150 mm turf and 50 mm insulation. Galvanized 13 mm steel pipe coils were buried in the roof slab with a pipe occupation ratio of 0.12. The walls were constructed of 240 mm common brick with 10mm cement plaster on the inside and outside surfaces and 20 mm Styrofoam insulation on the inside surface and covered with PVC panel. Thermistors were used to measure the indoor and outdoor temperatures, TAR system water inlet and outlet temperatures and temperature distribution inside the concrete slab. The effect of pipe spacing and water mass flow rate were evaluated. Agreement was good between the experimental and RC-thermal model. Concrete core temperature reaches the supply water temperature faster for lower pipe spacing. Heat extracted from the space increased with water mass flow rate to an optimum of 0.0088 kg/s.m².

Keywords: concrete core conditioning, thermally activated roof, RC- thermal model, thermo-active building simulation.

نموذج رياضي لمنظومة تبريد باستخدام سقف محفز حراريا باستخدام موديلRC الحراري المبسط باستخدام ماء متغير درجة الحرارة مع الوقت.

د. خالد احمد جودي
استاذ
كلية الهندسة - جامعة بغداد
قسم الهندسة الميكانيكية

كمال محمد علي
طالب دكتوراه
كلية الهندسة - جامعة بغداد
قسم الهندسة الميكانيكية

الخلاصـــــة

يستعرض هذا البحث نموذج محاكاة باستخدام الحاسوب للسقوف المنشطة حراريا (TAR) باستخدام ماء بارد من برج تبريد من النوع الرطب. تمت النمذجة باستخدام ما يسمى دائرة المقاومة- المتسعة الحرارية (نموذج RC) لسطح متناهي الابعاد. أعتبر انتقال الحرارة من شبكة الانابيب, ثنائي البعد (2-D) حيث نحتاج الى عدد قليل من العقد(nodes) للحصول على نتائج واقعية. أن استخدام النمذجة الحرارية (RC) من الرتبة السادسة سينتج عنه مجموعة من المعادلات التفاضلية الاعتيادية التي تم حلها باستخدام برنامج ماتلاب (Matlab R2012a). تمت صياغة البرنامج بحيث يغطي كل الاحتمالات الممكنة من ظروف ابتدائية و نوع مواد البناء و ابعاد منظومة TAR و التغير الزمني في شدة الاشعاع الشمسي. أعتبر الماء البارد المجهز متغير درجة الحرارة بسبب التغير الزمني لدرجة الحرارة الرطبة للهواء الخارجي. قورنت النتائج المتحصلة من النمذجة الحرارية(RC)مع النتائج العملية المستخلصة من غرفة تقع في الطابق الثاني ذات ابعاد 5.5 x 4 x 3 م في مدينة العمارة جنوب العراق (31.865 ˚N, 47.128 ˚E). يتركب السقف من 200 ملم خرسانة و 50 ملم عازل حراري و 150 ملم تراب. دفنت اربع شبكات انابيب من الحديد المغلون بقطر 13 ملم داخل الصبة الخرسانية للسقف مع نسبة اشغال انابيب بلغت 0.12. تتركب الجدران من 240 ملم طابوق عادي مع 10 ملم سمنت على جانبي الجدارين الداخلي و الخارجي و 20 ملم عازل الستايروفوم من الداخل الذي تم تغليفه بصفائح البلاستك الملونة. استخدمت متحسسات لقياس درجة حرارة الهواء الداخلية و الخارجية و درجة حرارة الماء الداخل و الخارج من منظومة TAR و التوزيع الحراري داخل الخرسانة. تمت دراسة تأثير التباعد بين الانابيب و الموقع العمودي لشبكة الانابيب داخل الخرسانة و تأثير معدل جريان الماء على اداء المنظومة. وجد ان هناك تطابق جيد بين النتائج العملية و تلك المتحصلة من نموذج RC الحراري وقد اعطى استخدام هذا النموذج نتائج قريبة من القياسات العملية. ان اقتراب درجة حرارة الخرسانة من درجة حرارة الماء المجهز يكون اسرع عند تباعد انابيب بمسافات اصغر. ازدادت الحرارة المسحوبة من الغرفة مع زيادة معدل جريان الماء الى 0.0088 كغم/ثا.م^2 و بعدها كان هناك تغير طفيف.

الكلمات الرئيسية: تكييف كتلة الكونكريت, سقف مثار حراريا, نموذج حراري, محاكاة البنايات المحفزة حراريا.

1. INTRODUCTION

Concrete core conditioning (CCC) is a system of thermal conditioning of buildings which uses water pipes embedded in the center of the floor/ceiling construction for heating and cooling, **Rietrkerk, 2010**. Water provided to CCC systems is provided by refrigeration, boiler, ground coupled source or any other low or high grade energy source at a temperature within a preset control limit. Recently, it has been used as an alternative for conventional installations and emerged as an energy efficient and cost effective system that realizes a good thermal indoor environment, **Koschnez and Lehmann, 2000**. These systems are mainly used in multistory office buildings with a low heating load in winter (10 to 30 W/m^2) and a moderate cooling load in summer (30 to 60 W/m^2), **Olesen, 2002**. Conductive, convective and radiative heat transfer all play an important role in describing the thermal behavior of CCC in buildings.

A TAR system is one of the CCC systems activated with water through pipes embedded in the concrete structure. Numerical simulation models can provide solutions to complex dynamic systems of buildings and technical installations, **Karlson, 2006**. Very often, a numerical solution is adopted to calculate 3D or 2D models for the temperature distribution in the concrete slab of a CCC building. Heat transfer processes are time dependent and change with the use of the building, the outdoor climate and the supply of cold/hot water to the building integrated cooling/heating system. **Sourbroun, 2012** used a finite difference method to model a full CCC system. **Antonopoulos and Tzivanidis, 1997** compared a 3-D and 2-D FD-method with experimental results. **Russell, and Surendran, 2001** used an FD-model to analyze the cooling capacity and perform some parametric analysis. **Olesen et al., 2006** presented an FD-model which is incorporated in the European standard EN15377 on water based embedded heating and cooling systems. A commonly used method to describe transient heat transfer in a multi-layer material is the thermal Resistance-Capacitance or RC-model. It is a simplified model where thermal resistances and capacities are lumped in a small number of nodal points **Weber, and Johannesson, 2005**. **Pedersen et al., 2005** used a 'space mapping' technique to optimize the performance of a computationally inexpensive RC network model. A detailed Finite Control Volume (FCV) model was used to enhance the accuracy of the simplified RC model. Furthermore, nothing was found regarding circulation of cooled water produced by a wet cooling tower, or hot water produced by an evacuated glass tubes solar collectors through embedded pipes in concrete slabs, neither experimentally (prototype or full scale) nor by using simulation packages, for residential comfort.

2. SYSTEM DESCRIPTION

2.1 Room Description

The room that was constructed to evaluate the mathematical model was located in the second story of a residence located in Amarah city/ south of Iraq (31.865 ˚N, 47.128 ˚E). It measures 5.5 m x 4 m x 3 m as shown in **Fig. 1**. The roof was constructed of 200 mm heavyweight concrete, 50 mm insulation and 150 mm turf which is a conventional roof construction in the south of Iraq. Walls were constructed of 240 mm common brick and finished with 10 mm cement plaster on both sides with 20 mm Styrofoam insulation on the inside and covered with a PVC panel as an architectural wall siding material. The external steel door included a double glazed aperture measuring 1 m x 1m with a 10 mm air space. Infiltration through door cracks is minimized by air tight gaskets. Opaque venetian blinds were used as an external shading device. A 400 mm overhang shaded the eastern wall and external door. The ground floor below the room was conditioned.

2.2 TAR system description

The TAR system was constructed of 13 mm galvanized steel pipes embedded in the 200 mm concrete slab with 170 mm pipe spacing. **Fig. 2** is a section through the room showing the cooling tower and temperature sensor locations. Pipe coils were located 80 mm above the bottom side of the concrete slab. Therefore, the pipe deepness ratio is 0.4. The pipe deepness ratio can be defined as the ratio between the pipe level height to the concrete thickness. The TAR system included four pipe coils with the option of either parallel or series connection. **Fig. 3** shows the piping system and the external connections. Each coil pipe pass was 5.5 m long. Anti-corrosion paints were used on the outside of these pipes. Water pipe loops were attached to the steel reinforcement bars firmly to prevent them from floating during concrete pouring. Lime stone was added to the concrete mix to prevent steel corrosion, **Verlmon, 2008**. The percentage of total surface area of the pipes to the effective area of the roof is defined as the pipe occupation ratio index which was 12 % for this roof. A wet cooling tower of 2 kW capacity, 0.206 l/sec and L/G = 0.623 was designed and constructed at 22 °C design wet bulb temperature and 4 °C approach to provide cold water to the TAR system. Cold water to the TAR system made the concrete slab a heat sink panel. The system water was treated with Potassium Dichromate tablets to prevent pipe corrosion and phenol to prevent algae and other green living forms.

2.3. Instrumentation and Measurements

Temperature measurements were made using 14 temperature calibrated thermistors type LM35. This type does not require any calibration or trimming to provide typical accuracies of ±0.25˚C at room temperature. Eight of them were distributed across the roof span between pipes to measure the temperature distribution across the concrete. Another four, were used to measure the indoor and outdoor dry and wet bulb temperatures. Two sensors were used to measure the inlet and outlet water temperatures across TAR (cooling tower) system. These sensors were connected to a data acquisition system manufactured by Lab-Jack company of Lakewood, Colorado, USA, model U3 LV. Data were saved in spread sheet format. A rotameter 2-26 l/min with accuracy of $\pm$ 3.14 % manufactured by SKC, was installed to measure the water flow rate in the system. System power consumption was measured by an (A-V-O) digital clamp meter supplied by Fluke 323 company with current and voltage range of 0-400 A with an accuracy of 1.5 $\pm$ 5 % and a voltage range of 0-750 V with accuracy an of 2 $\pm$ 5 %.

3. COOLING LOAD ESTIMATION

Olesen, 2002 suggested that thermally activated systems are suitable for buildings with moderate cooling loads of approximately 30 W/m² to 60 W/m². Several modifications were applied to decrease the cooling load of this test room. The heat gain was minimized using thermal insulation, air tight sealing, double glazing, external shading and an overhang.

Internal heat sources were limited to a 45 W lighting and a ceiling fan of 60 W powers. The Space cooling load was maximum on 21 July at a value of 51.6 W/m² which is a moderate value and suitable for TAR system installation. **Fig. 4** shows the cooling load of the space using the radiant time series (RTS) method for 21 July **ASHRAE, 2009**. The exterior glazed door has a peak cooling load in the morning because it faces east while walls and roof have a peak load at night due to the thermal mass storage of these structures. The total load is of a maximum near mid-night.

4. RC-THERMAL MODELLING

Hourly temperature distribution through the roof layers was determined using a simplified RC thermal network. Input temperatures to the model were from experimental measurements of the test room for 21 July as shown in **Fig. 5**. Other input data include the solar radiation intensity and supply water temperature. Input data included the material thermal properties and water flow rate which are independent of time. Six nodes were used across the roof thickness which rendered a 6^{th} order model. The internal nodal points have thermal capacities. Whereas, the surface nodal point thermal capacities are set to zero. Modeling was carried out with the experimental data of 21 July, 2013 as input.

A general sinusoidal equation for nodal temperatures introduced by Joseph, 2012 is used in the present model as;

$$T_{ml} = T_m + A \sin(2\pi/24\,(t \pm \emptyset)) \quad (^{\circ}C) \quad (1)$$

$$T_m = (T_{max}+T_{min}) / 2, \quad (^{\circ}C) \quad (2)$$

$$A = (T_{max} - T_m), \quad (^{\circ}C) \quad (3)$$

Where $\emptyset$ is the phase shift (hr), and $\pm$ signs are for descending and ascending directions.

4.1 Temperature Modeling

The sol-air temperature, outdoor, indoor and supply water temperature were modeled for computer program implementation.

The sol-air temperature is a fictitious temperature that defines a value for the outdoor air temperature which would, in the absence of all radiation exchanges, give the same rate of heat flow into the outer surface as the actual combination of temperature difference and radiation exchanges, **Kreider et al., 2002**. It takes into account, the daily temperature range which affects the heat storage, the color of the outside surface which affects solar heat absorption rate, the latitude and month, **Duffie, 2006**. In equation form;

$$T_e = T_{do} + \alpha \frac{I_t}{h_o} - \frac{\varepsilon \Delta R}{h_o} \quad (4)$$

The solar irradiance is given as;

$$I_t = 0, \quad (1 \le t \le 6) \tag{5}$$

$$I_t = 980 \sin(2\pi/24\,(t-6)), \quad (6 \le t \le 18) \tag{6}$$

$$I_t = 0, \quad (18 \le t \le 24) \tag{7}$$

Where 980 W/m² was the maximum total solar radiation calculated on a horizontal surface for 21 July at Amarah city **ASHRAE, 2009** assumes the following equation to evaluate the sol-air temperature for horizontal surfaces,

$$T_e = T_{do} + 0.026\, I_t - 4 \quad (°C) \tag{8}$$

From experimental data of 21 July, 2013 and Eq.(1), the ambient dry bulb temperature T_{do}, ambient wet bulb temperature T_{wo}, indoor dry bulb temperature T_{di} and cooling water supply temperature T_s with an approach of 4 ˚C, can be written as;

$$T_{do} = 38 + 8 \sin(2\pi/24(t-8)), \quad (1 \le t \le 24) \quad (°C) \tag{9}$$

$$T_{wo} = 21 + 4 \sin(2\pi/24(t-8)), \quad (°C) \tag{10}$$

$$T_s = 25 + 4 \sin(2\pi/24(t-8)) \quad (°C) \tag{11}$$

$$T_{di} = 30.3 + \sin(2\pi/24(t+6)) \quad (°C) \tag{12}$$

Fig. 6 compares the experimental measurements of the outdoor temperature and Eq. (9).

So, sol-air temperature is modeled using Eqs. (5), (6), (7), (8) and (9) as;

$$T_e = 38 + 8\, sin(2\pi/24(t-8)) + 0.026\, I_t - 4, \quad (°C) \tag{13}$$

4.2 TAR system modeling

The roof slab was regarded as an infinite slab with four internal nodal points and two for the upper and lower surfaces. The governing equations for typical exterior and interior nodes shown in **Fig. 7** are:

Exterior node 1; $$0 = \frac{1}{R_o}(T_e - T_1) + \frac{1}{R_1}(T_2 - T_1) \tag{14}$$

Internal node 3; $$C_2 \frac{dT_3}{dt} = \frac{1}{R_2}(T_2 - T_3) + \frac{1}{R_3}(T_4 - T_3) \tag{15}$$

For node 4; $$C_3 \frac{dT_4}{dt} = \frac{1}{R_3}(T_3 - T_4) + \frac{1}{R_5}(T_6 - T_4) + \frac{1}{R_4}(T_5 - T_4) \tag{16}$$

For the pipe node 5; $C_5 \frac{dT_5}{dt} = \frac{1}{R_4}(T_4 - T_5)$ (17)

Where, C_5 is the thermal capacitance of the pipe material.

Replacing $\frac{dT}{dt}$ by $\frac{\Delta T}{\Delta t} = \frac{(T^{new} - T^{old})}{\Delta t}$ and solving the resulting equation system, the following matrix equation evolves;

[A][T]= [B] (18)

Where [A] is the thermal coefficient matrix, [T] is the new temperatures matrix and [B] is the old temperatures matrix.
The resistance R_5 is 3-dimensional but may be given as a 1-dimensional relation as, **sourbroun, 2012**;

$$R_5 = \frac{S \ln\left(S/\pi d\right)}{2\pi k_p} \quad (19)$$

The main concept in TAR geometry is shown in **Fig. 8**.

Where : $l_4/(l_3 * s) > 0.3,\ d/s < 0.2$.
The temperature at node 5 is assumed the same as the pipe temperature and can be related to the supply water temperature by;

$$\dot{q}_{wr} = \dot{m}\ c_p(T_r - T_s), \quad \text{(W)} \quad (20)$$

$$\text{And, } \dot{q}_{4-5} = \frac{(T_4 - T_5)}{R_5} \quad \text{(W)} \quad (21)$$

By assuming a linear temperature rise along the pipe length, the pipe temperature can be approximated as;

$$T_5 \cong \frac{T_s + T_r}{2}, \quad (^{\circ}C) \quad (22)$$

Solving Eqs. (20), (21) and (22) gives;

$$T_5^{old} = T_s - \frac{1}{2}\left(\frac{\frac{1}{R_5}(T_5^{old} - T_4^{old})}{\dot{m}\ c_p}\right) \quad (^{\circ}C) \quad (23)$$

Substituting Eq. (11) in Eq. (23) gives;

$$T_5^{old} = 25 + 4\sin\left(\frac{2\pi}{24}(t-8)\right) - \frac{1}{2}\left(\frac{\frac{1}{R_5}(T_5^{old} - T_4^{old})}{\dot{m}\ c_p}\right) \quad (^{\circ}C) \qquad (24)$$

So, T_5^{old} was calculated each time interval iteratively to determine the pipe temperature at node 5. The thermal resistances (R) and capacitances (C) are parameters with constant values that are based on the properties of each of the construction layers as;

$$C = \rho c_p V \qquad (J/^{\circ}K) \qquad (25)$$

Performance of TAR system can be evaluated once the node temperatures at each time step are determined. The rate of heat transferred between the roof and the water supplied to the TAR system is calculated as;

$$\dot{q}_{tr} = \dot{m}\, c_p (T_r - T_s) \qquad (W) \qquad (26)$$

Or, the heat extracted from the concrete slab by the TAR piping system can be calculated as;

$$\dot{q}_c = \pi d\, L\, (T_4 - T_5)/R_5 \qquad (W) \qquad (27)$$

The heat extracted from the room by the TAR system across the lower roof surface, can be calculated as;

$$\dot{q}_i = h_i A\ (Ti - T6) \qquad (W) \qquad (28)$$

The rate of heat transferred from the upper roof surface transmitted to the surrounding and is calculated as;

$$\dot{q}_{sur} = h_o A\ (T_e - T_1) \qquad (W) \qquad (29)$$

TAR system instantaneous efficiency η_{TAR}, in this work is defined as the ratio of the heat extracted from the room by the TAR system to the heat extracted from the concrete slab by the cooled water as;

$$\eta_{TAR} = \dot{q}_i/\dot{q}_c \qquad (30)$$

Effectiveness of the TAR system is defined as the ratio of the heat extracted from the concrete slab by the cool water to the mechanical power spent to drive the TAR system as **Sourbroun, 2012**;

$$\in_{TAR} = \dot{m}\, c_p (T_r - T_s)/P_{con.} \qquad (31)$$

$$P_{con.} = A_l * V_l * (P.F) * \eta_b \qquad (W) \qquad (32)$$

Where: $P_{con.}$ is the power consumed in driving the cooling tower fan and pump, P.F is the power factor = 0.75 and η_b is the brake efficiency which is assumed equal to 0.85 for tower fan and pump.

5. COMPUTER IMPLEMENTATION

Fig. 9 is a flow chart of the main procedures in the computer model using for the Matlab program. Matlab R2012a computer program was used to solve the set of six linear algebraic equations. The program input command identifies the initial conditions, material thermal properties and geometry. Using the 'solve' Matlab command statement, the nodal temperatures are determined for a certain time step which then become old temperatures for the next time step except T_5^{old} which is calculated each time interval depending on the instantaneous supply water temperature. A time step of 1800 seconds (30 minutes) was used in this model. The 'Input' Matlab statement provides several initial conditions, several material properties and geometrical dimensions for system flexibility and to determine their effects on the temperature distribution through the concrete slab and the heat exchange rate with the piping network and surroundings.

6. RESULTS AND DISCUSION

6.1 Concrete temperature history

Fig. 10 shows the temperature history of the concrete core and the mean measured concrete temperature. The deviation is partly thought to be due to neglecting conduction in the pipe material and forced convection of water flow which were lumped as one parameter in T_5. Also, the assumption of linear rise of the supply water temperature could generate part of this discrepancy. The deviation of results between model and measured concrete temperature is depicted as a time lag of approximately one hour. Possibly, the thermal capacitance of components in the model do not account for this time lag. One of the more important results of the RC-thermal analysis is the hourly temperature distribution across the roof deck as shown in **Fig. 10**. Node positions in **Fig. 11** are at, 0 cm, 8 cm, 23 cm, 33 cm and 40 cm from the roof lower surface. They are nodes 1, 2, 3, 4 and 6 in the RC-network respectively. The amplitude of temperature variation is lower near the roof lower surface. This is due to the high thermal mass storage and insulation of the upper part of the roof. Temperature history of node 4, at the pipe level, shows the lowest amplitude due to the supply cold water temperature.

6.2 TAR system efficiency

TAR system efficiency varies with time due to the hourly variation of the ambient temperature, indoor temperature and slight variation of the cool supply water temperature. It is noted that efficiency attains values greater than unity as shown in **Fig. 12**. This is invalid because $\dot{q}_i < \dot{q}_c$. This occurs due to the time lag between the heat extracted by the concrete from the cool TAR water ($\dot{q}_c$) and the heat extracted from the room ($\dot{q}_i$). If this time lag is set to zero by slight modulation in **Fig. 12**, the efficiency takes the form shown in **Fig. 13**. Efficiency is of maximum at night. The rate of heat extracted from the space is of maximum at night when the cooling load is maximum. **Fig. 14** compares hourly cooling load $\dot{q}_{cl}$ and heat extracted from the room $\dot{q}_i$ which highlights the TAR system contribution to space cooling

load. It shows that the extracted heat from the space is larger than the instantaneous cooling load for the period 13:00 – 19:00 hrs.

6.3 TAR System Geometry Effect

The effect of pipe spacing on the hourly temperature distribution through the concrete slab was evaluated for spacing of 10, 12, 14, 16 and 18 cm. Supply water temperature T_s shown in **Fig. 15** is the model temperature of node 4. It is noticed that the change in spacing causes a change in temperature amplitude and time delay due to the change in thermal mass storage. Low spacing reduces the time needed to approach the supply water temperature. Also, the experimental temperature of the node 4 falls between the model temperature for 15 cm and 18 cm spacing which is an excellent verification of the model.

The effect of pipe deepness ratio in the heat extracted from the space by RC model and experimental measurements is shown in **Fig. 16.** The higher the ratio the lower the heat extracted from the space and vice versa. The experimental representation in this figure is illustrated as a single point due to the fixed deepness ratio of the present work. A small deviation was noted. This may be due to the using the mean water temperature to compute the heat extracted by RC model.

6.4 Effect of Water Mass Flow Rate

The water temperature and flow rate influence the thermal performance of the TAR system strongly. Lower water temperatures mean better performance as shown in **Fig.17**. Moreover, TAR system effectiveness increases with flow rate up to $\dot{m}$ = 0.0088 l/s.m² beyond which there is only a slight improvement as shown in the figure. It is more efficient to change the water supply temperature T_s than to increase the water flow rate.

7. CONCLUSIONS

Based on the results the following conclusion can be drawn:

1- There is a small deviation between concrete nodal temperatures obtained by the RC-model and the measured temperatures at spacing of 17 cm.
2- TAR effectiveness improves significantly with lower supply water temperature and only slightly with increased water flow rate beyond 0.0088 l/s.m².
3- Increasing pipe spacing causes an increase in concrete temperature amplitude and time shift.
4- The heat extracted from the space decreased with pipe deepness ratio.

REFERENCES

- Antonopoulos, K. A., Tzivanidis, C. G., 1977, *Numerical Solution of Unsteady Three-Dimensional Heat Transfer during Space Cooling using Ceiling Embedded Piping.* In Energy, Elsevier, Vol. 22, No. 1, pp. 59-67.

- ASHRAE Handbook, Fundamentals, ASHRAE, Inc., Atlanta, GA, USA, 2009.

- Duffie A. and Beckman W. A., 2006, *Solar Engineering and Thermal Process*, Third ed. John Wiley and Sons, New York .

- Joseph M., 2012, *Calculus for the Life Sciences II Lecture, Notes – Trigonometric Functions*. Department of Mathematics and Statistics Dynamical Systems Group Computational Sciences Research Center, San Diego, State University San Diego.

- Karlson J. H., 2006, Thermal system analysis of embedded building integrated heating. thesis for the degree of licentiate of engineering, Department of Civil and Environmental Engineering, Chalmers University of Engineering, Göteborg, Sweden.

- Koschenz, M., and Lehmann, B., 2000, Thermo-active building systems TABS, EMPA Energiesysteme / Haustechnik, Duebendorf (Switzerland).

- Kreider S., Curtiss U., Rab L., 2002, *Heating and Cooling of Buildings*, 2nd ed., McGraw-Hill, New York, USA.

- Olesen W.B., 2002, *Control of Slab Heating and Cooling Systems Studied by Dynamic Computer Simulations*. Symposium, ASHRAE Transaction, V. 108, Pt. 2.

- Olesen, W., Carli, M. D., Scarpa, M., and Koschenz, M., 2006, *Dynamic Evaluation of the Cooling Capacity of Thermo-Active Building Systems*. ASHRAE Transactions 112, 2.

- Pedersen, F., Weitzmann, P. and Svendsen, S., 2005, *Modeling thermally active building components using space mapping*. Proceedings of the 7th Symposium on Buildings Physics in the Nordic Countries. Reykjavík, Iceland.

- Rietkerk J., 2010, *Evaluation of the Concrete Core Conditioning Performance for Flexible Building Zone Configurations*. 8th International conference on system simulation in buildings, Liege, (Paper P102), (pp. 20).

- Russell, M. B., and Surendran, P. N., 2001, *Influence of Active Heat Sinks on Fabric Thermal Storage in Building Mass*. Applied Energy 70, 17–33.

- Sourbroun M., 2012, *Dynamic Thermal Behavior of Buildings with Concrete Core Activation*. PhD thesis, Arenberg Doctoral School of Science.

- Vermolen F. J., 2008, *Predicting Critical Conditions for Bacterial Self-Healing of Concrete and Sand*. PhD thesis, Delft University of Technology, Delft Institute of Applied Mathematics, Mekelweg42628 CD Delft, The Netherlands.

- Weber, T., and Johannesson, G., 2005, *An Optimized RC-Network for Thermally Activated Building Components*. Building and Environment 40, 1–14. pages 23, 50, 89, 137, 140, 163.

NOMENCLATURE

A	temperature amplitude	(A)
A_l	line current	(A)
A_r	roof area.	(m^2)
C	capacitance.	(kJ/℃)
c_p	specific heat.	(kJ/kg. ℃)
d	diameter.	(m)
h	convective heat coeff.	($W/m^2.$ ˚C)
I_t	total solar radiation Intensity.	(W/m^2)
k	thermal conductivity.	(W/m.˚C)
l	thickness.	(m)
L	pipe Length.	(m)
$\dot{m}$	mass flow rate	(kg/s)
P	power.	(W)
$\dot{q}$	heat transfer rate.	(W)
R	thermal resistance.	(m^2. ˚C/W)
ΔR	the difference between incident and emitted radiation from black body.	(W/m^2)
s	spacing.	(m)
T	temperature.	(˚C)
T_e	sol-air temperature.	(˚C)
t	time.	(s)
V	volume	(m^3)
V_l	line voltage	(Volt)
w	slab width.	(m)

Greek symbols

α	surface absorptance.
ε	surface emittance.
$\in_{TAR}$	TAR effectiveness.

$\emptyset$	phase shift.	(hr)
η_b	brake efficiency.	
η_{TAR}	TAR efficiency.	
ρ	density.	(kg/m^3)

Subscripts

c	concrete.
con.	consumed.
d	dry bulb
i	indoor.
cl	cooling load.
max	maximum.
min	minimum.
m	mean.
ml	model.
o	outdoor.
p	pipe.
r	return.
s	supply.
sur	surround.
w	wet bulb
wr	water

Abbreviations

CCC	concrete Core Conditions.
FD	finite difference.
FCV	finite control volume.
PVC	poly vinyl chloride.
RC	resistance capacitance.
RTS	radiant time series.
TAR	thermally Activated Roof.

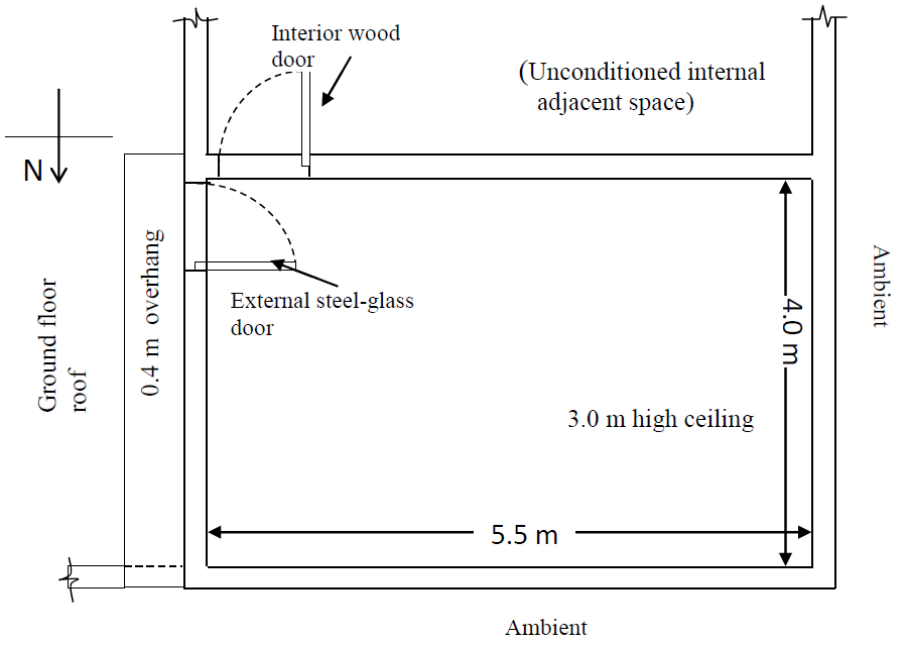

Figure 1. Plan view of the experimental room.

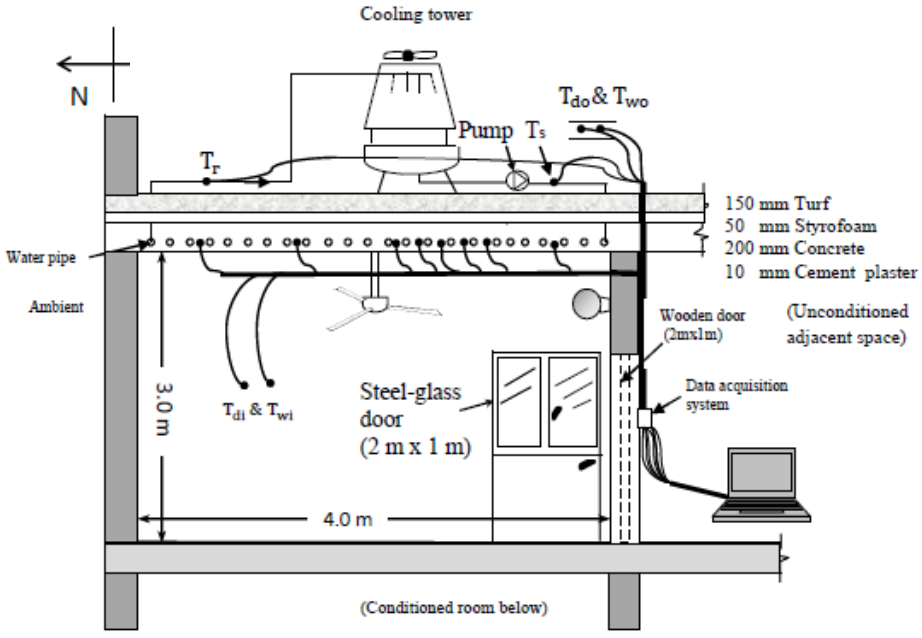

Figure 2. A front section of the test room. (•) temperature sensor.

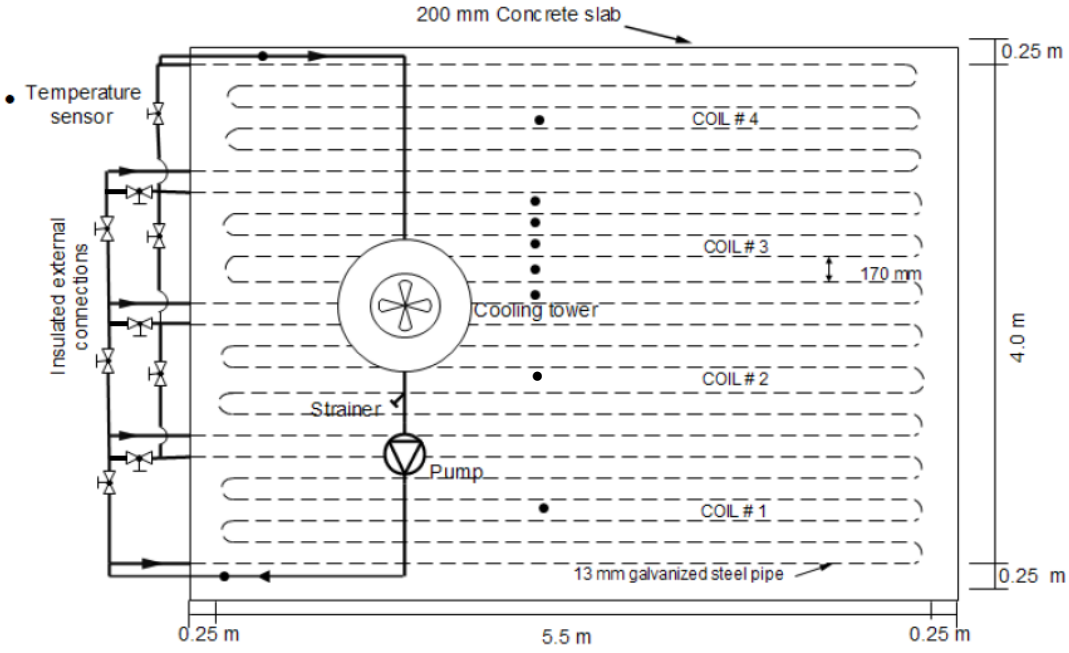

Figure 3. Pipe coils of the TAR system with coils external connections.

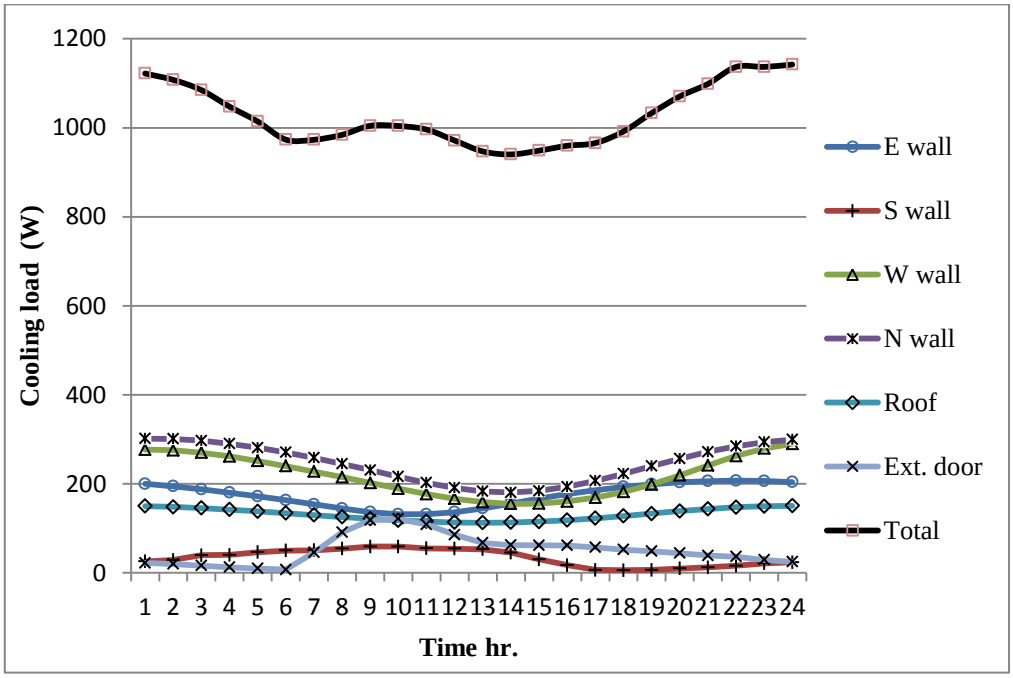

Figure 4. Cooling load components of the test room on 21 July.

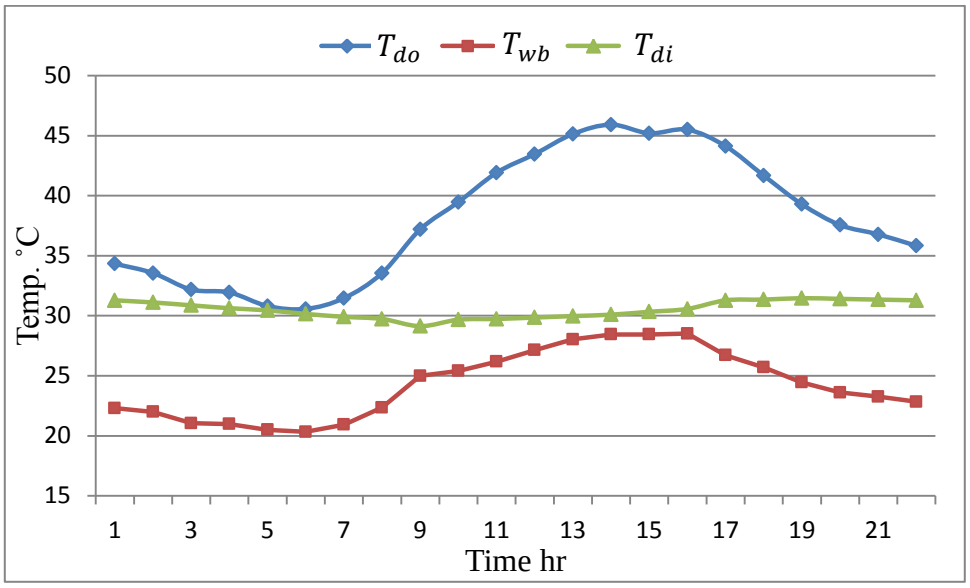

Figure 5. Experimental temperature measurements for 21 July, 2013.

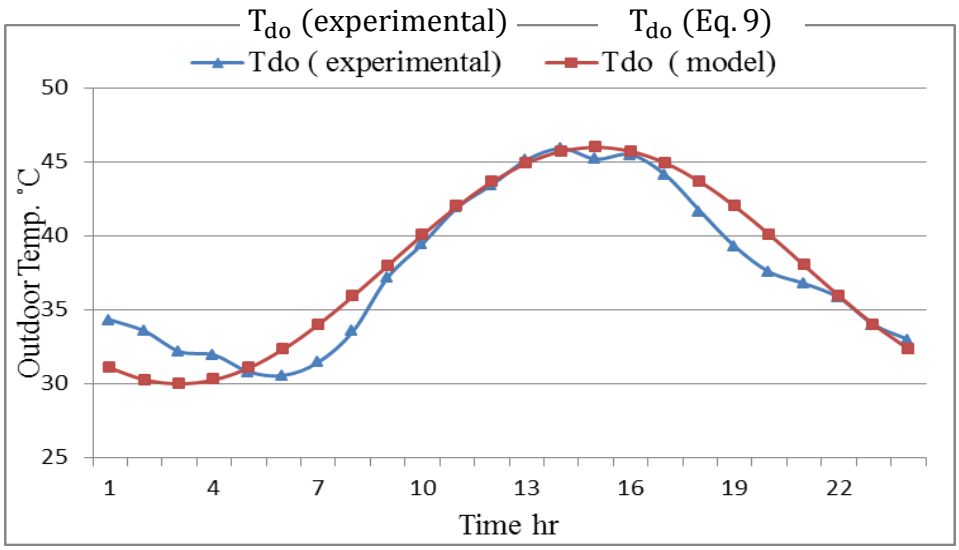

Figure 6. Experimental and model outdoor temperature profile.

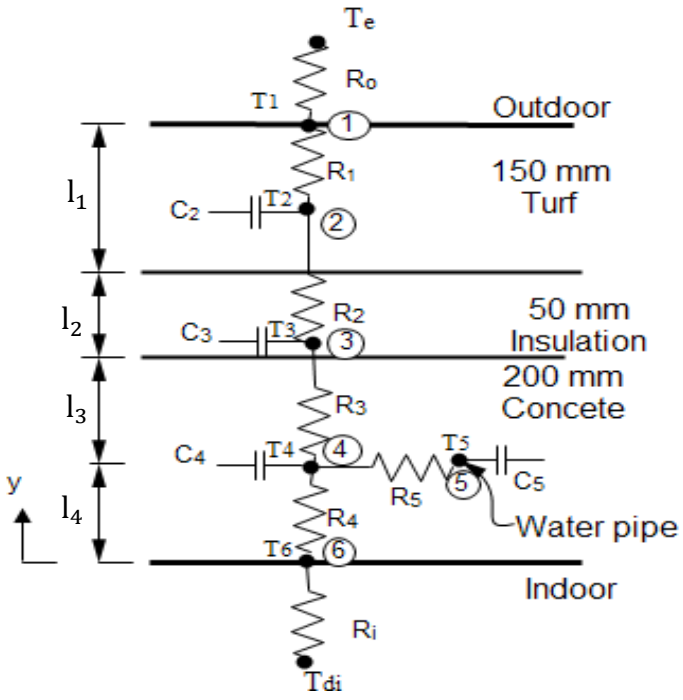

Figure 7. RC-thermal network model.

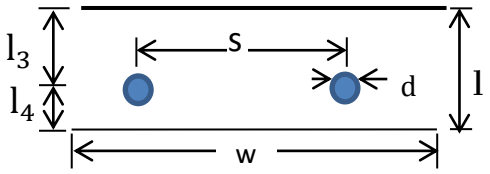

Figure 8. TAR geometry concept.

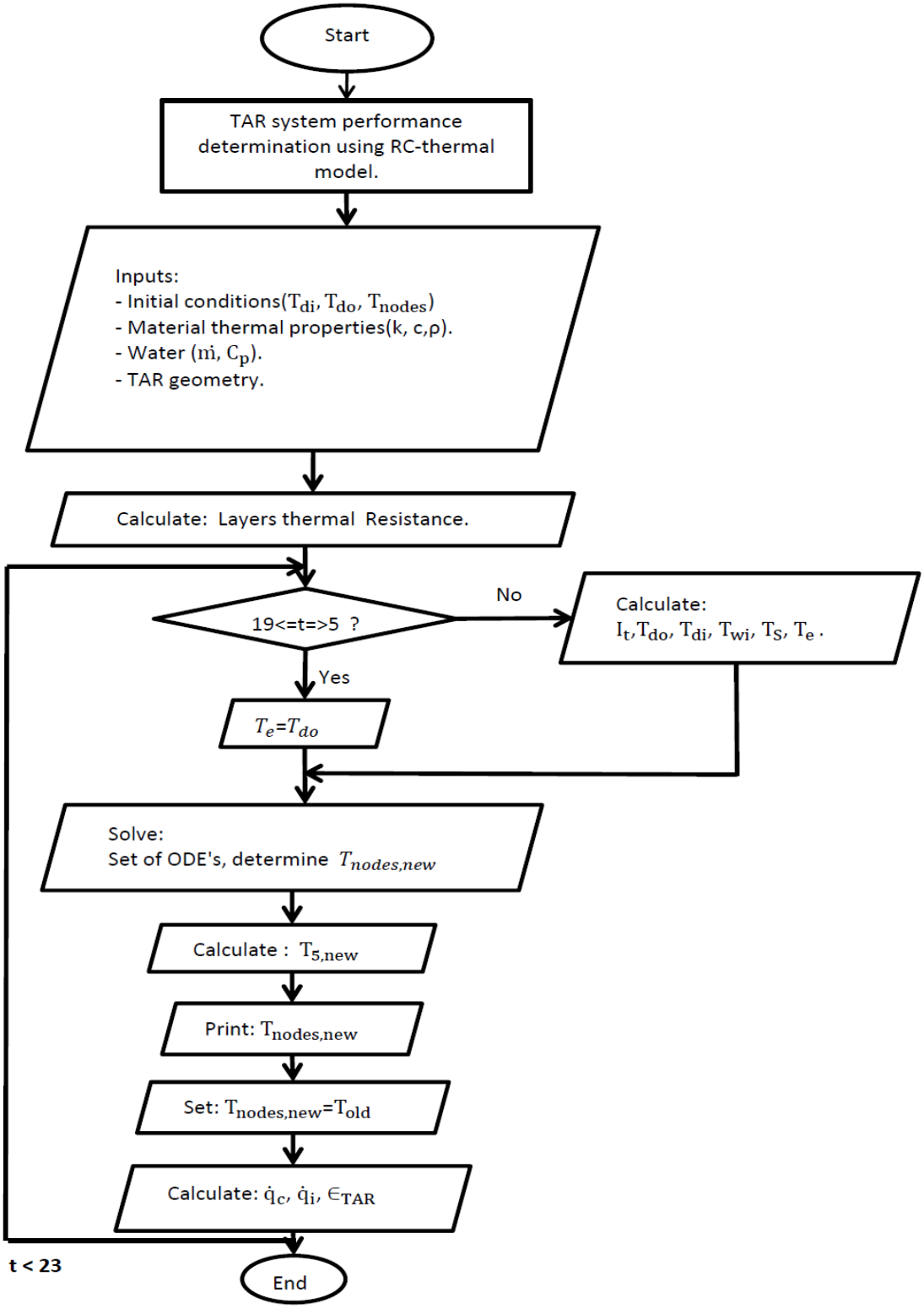

Figure 9. Flow chart of the computer model.

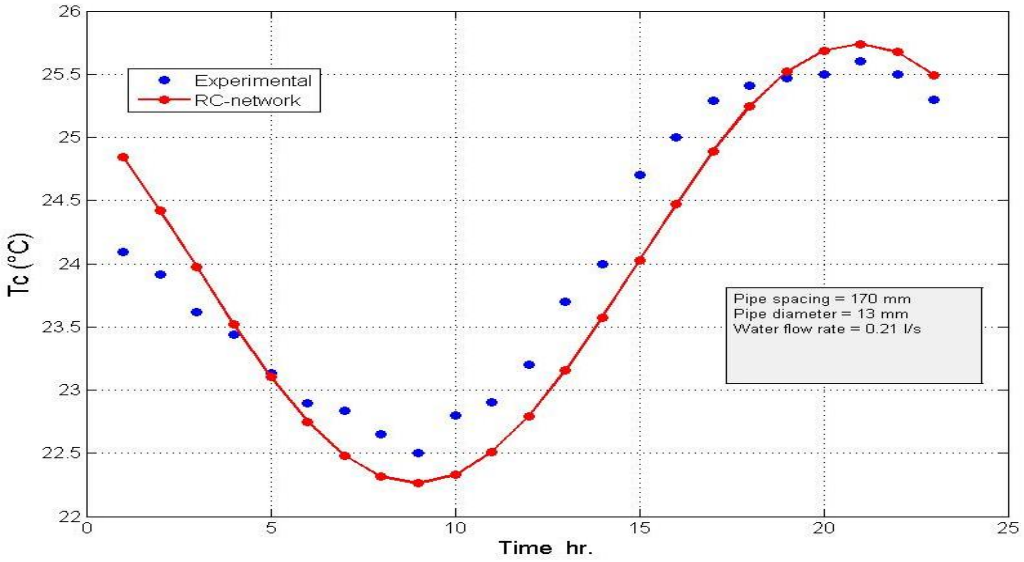

Figure 10. Concrete core temperature history.

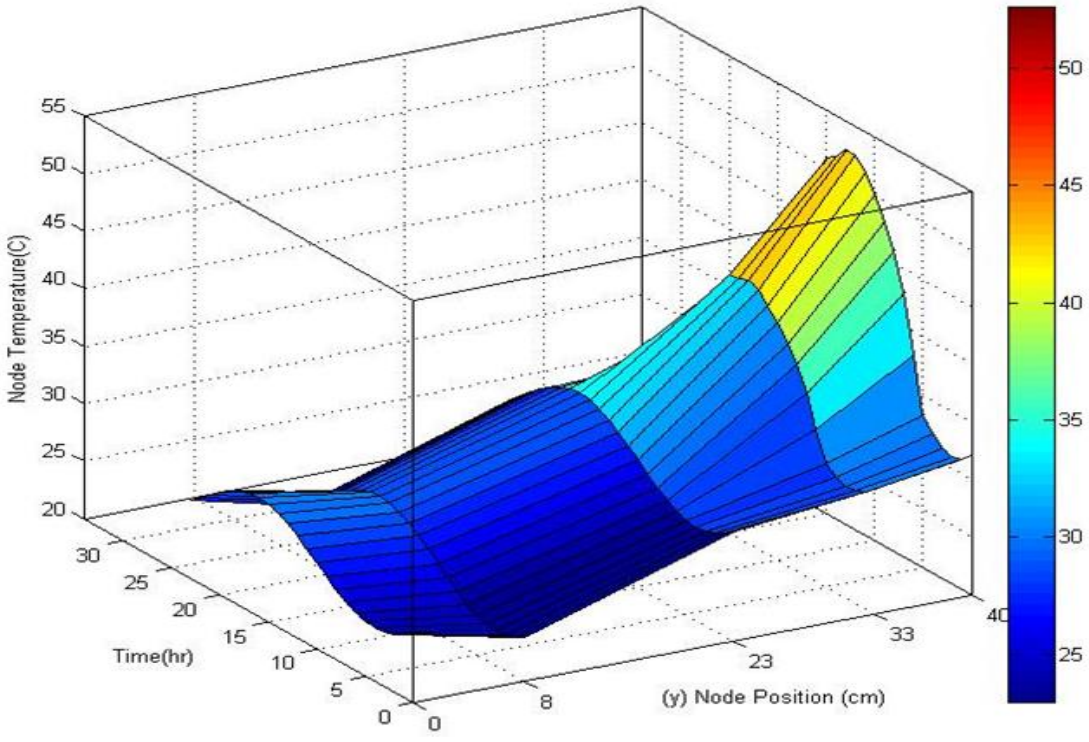

Figure 11. Nodal temperatures variation with time.

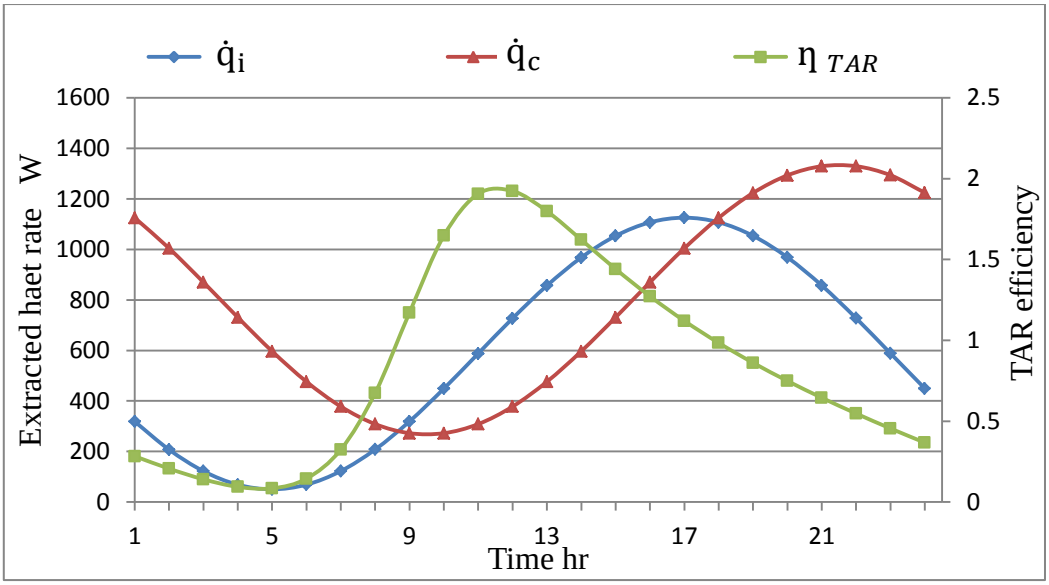

Figure 12. The effect of time lag on TAR efficiency.

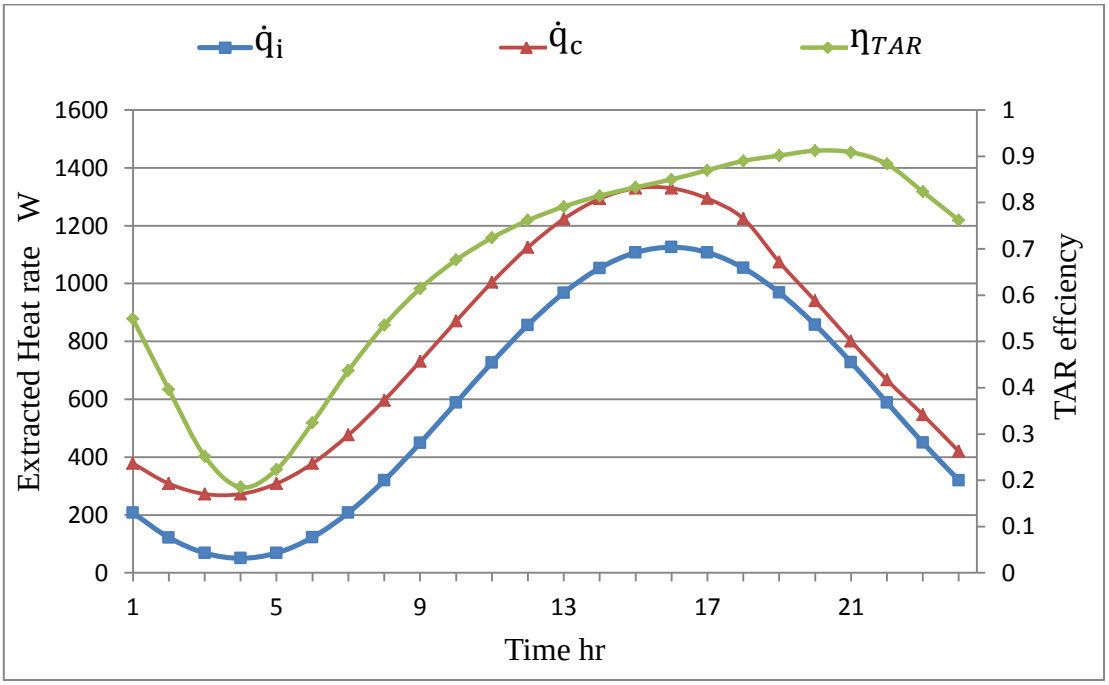

Figure 13. TAR system efficiency when time lag is set to zero.

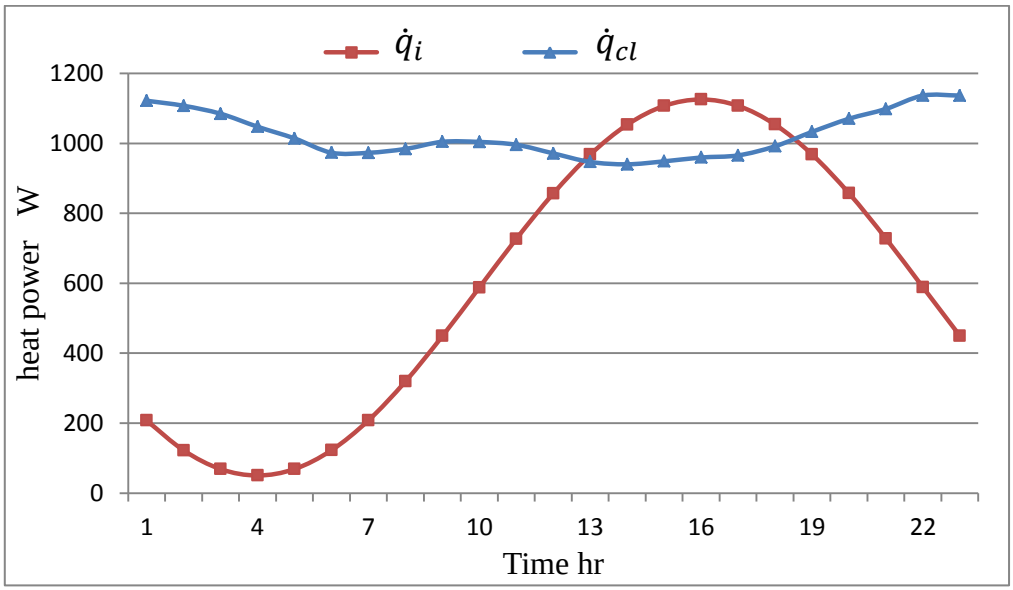

Figure 14. TAR system contribution in the heat extracted by TAR system compared with space cooling load on 21 July.

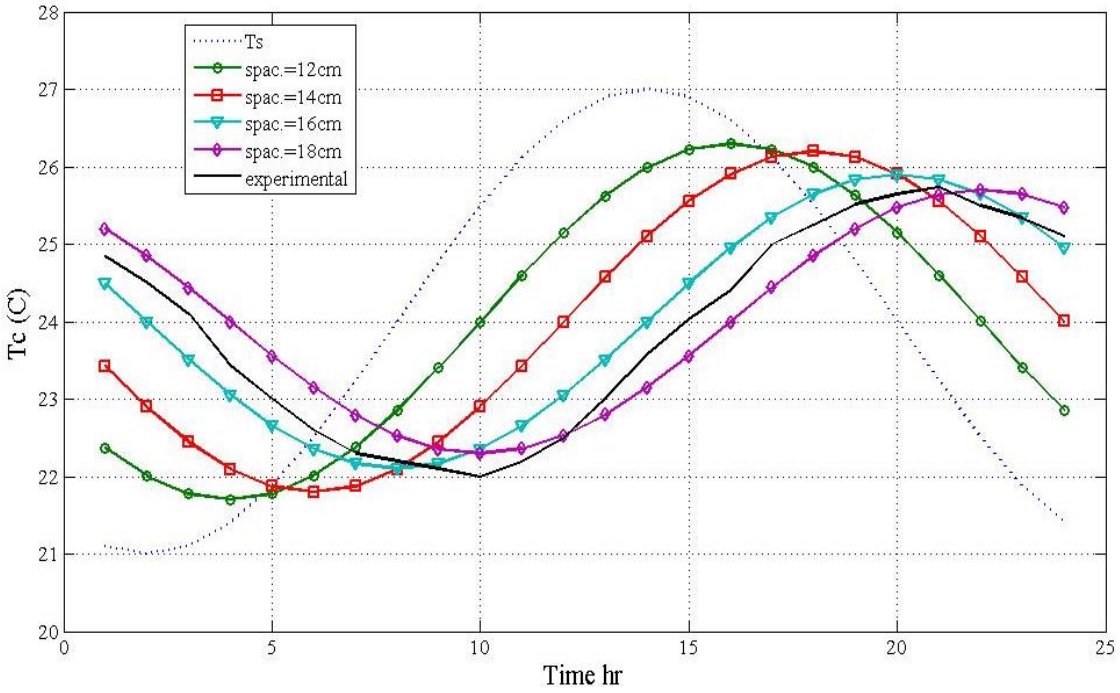

Figure 15. Pipe spacing effect on concrete temperature at node 4.

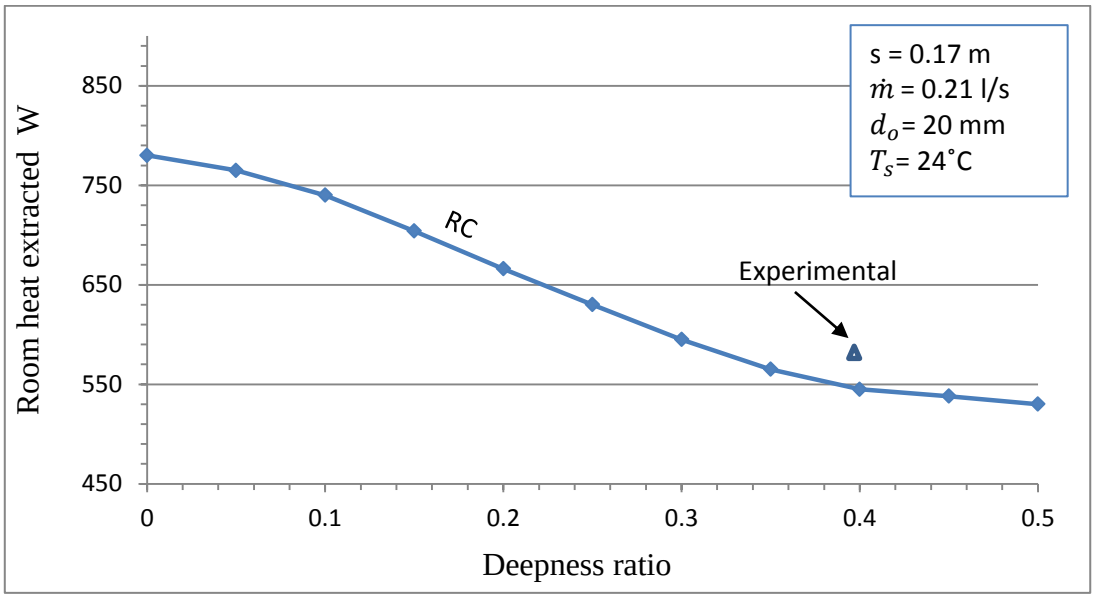

Figure 16. The pipe deepness ratio effect on the heat extracted from the space.

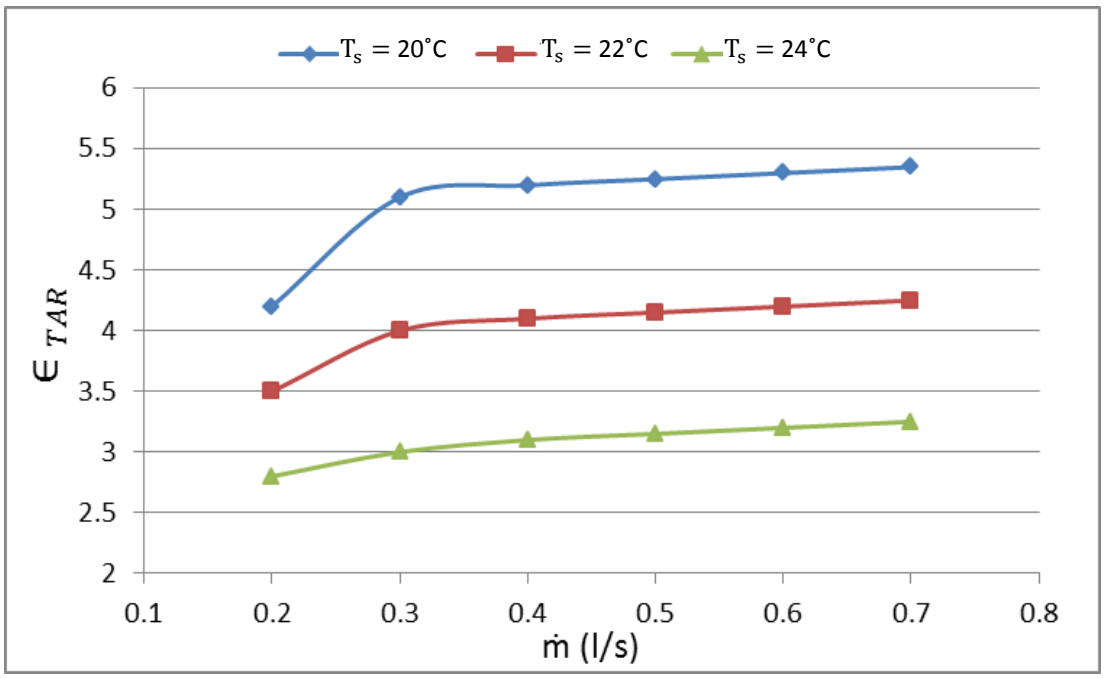

Figure 17. The effect of water mass flow rate and water supply temperature on TAR system effectiveness.